Hindawi Publishing Corporation
EURASIP Journal on Wireless Communications and Networking
Volume 2010, Article ID 751520, 13 pages
doi:10.1155/2010/751520

Research Article

Low-Complexity One-Dimensional Edge Detection in Wireless Sensor Networks

Marco Martalò and Gianluigi Ferrari

WASN Laboratory, Department of Information Engineering, University of Parma, I-43124 Parma, Italy

Correspondence should be addressed to Marco Martalò, marco.martalo@unipr.it

Received 16 February 2010; Accepted 26 May 2010

Academic Editor: Osvaldo Simeone

In various wireless sensor network applications, it is of interest to monitor the perimeter of an area of interest. For example, one may need to check if there is a leakage of a dangerous substance. In this paper, we model this as a problem of one-dimensional edge detection, that is, detection of a *spatially nonconstant* one-dimensional phenomenon, observed by sensors which communicate to an access point (AP) through (possibly noisy) communication links. Two possible quantization strategies are considered at the sensors: (i) binary quantization and (ii) absence of quantization. We first derive the minimum mean square error (MMSE) detection algorithm at the AP. Then, we propose a simplified (suboptimum) detection algorithm, with reduced computational complexity. Noisy communication links are modeled either as (i) binary symmetric channels (BSCs) or (ii) channels with additive white Gaussian noise (AWGN).

1. Introduction and Related Work

Sensor networks have been an active research field in the last years [1]. In particular, many civilian applications have been developed on the basis of this technology, for example, for environmental monitoring [2]. Several frameworks have been proposed for the analysis of sensor networks with a common binary phenomenon under observation [3–6]. While there are scenarios where the presence of a common phenomenon is meaningful, in other scenarios one may be interested in determining where the physical phenomenon changes its status (e.g., from presence to absence, or vice versa). As an illustrative example, consider the scenario shown in Figure 1(a). Suppose that in a given area there is a chemical facility where a dangerous gas is used. Obviously, it is of interest to detect any gas leakage. To this purpose, one may place a linear sensor network surrounding this area: in the example in Figure 1(a) there are six sensors. (In the remainder of this paper, by "sensor" we will denote the wireless transceiver which includes the sensing element. However, it has also (limited) processing capabilities and can communicate with the AP.) At a given time, it may happen that there is a leakage: some of the sensors (namely, sensors s_2, s_3, s_5, and s_6 in Figure 1(b)) thus detect the presence of the gas (namely, sensors s_2, s_3, s_5, and s_6) whereas the remaining sensors (namely, s_1 and s_4) do not. This problem reduces to a distributed detection problem of a spatially nonconstant binary phenomenon, as shown in Figure 1(c) and described in more detail later. We remark that this is an illustrative example of a possible one-dimensional edge detection application. Our goal is to show how low-complexity distributed detection can be successfully applied to solve a general one-dimensional edge detection problem.

In [7], the authors consider a scenario with a single phenomenon status change (denoted, in the following, as *edge*) and propose a framework, based on minimum mean square error (MMSE) estimation, to determine the position of this edge. In [8], under the assumption of proper regularity of the observed edge, a reduced complexity MMSE decoder is proposed. In [9], the authors show that an MMSE decoder is unfeasible for large-scale sensor networks, due to its computational complexity, and propose a distributed detection strategy based on factor graphs and the sum product algorithm. Moreover, MMSE-based distributed detection schemes have also been investigated in scenarios with (i) a common binary phenomenon under

observation and (ii) bandwidth constraints [10]. In [11, 12], the authors examine the problem of determining edges of natural phenomena through proper processing of data collected by sensor networks. In these papers, particular attention is devoted to the estimation accuracy, given in terms of the confidence interval of the results obtained with the proposed framework.

The problem of edge detection is also well known in the realm of image processing, where it may be of interest to characterize the intensity changes in the processed image. In [13], the authors characterize, from a theoretical point of view, the types of possible intensity changes. In [14], using numerical optimization, optimal operators are preliminary derived for ridge and roof edges, and then specialized for step edges. In [15], the edge detection problem is tackled as a statistical inference problem. Other interesting approaches to edge detection, especially for noisy information fusion scenarios, are proposed in [16, 17].

In [18], we have proposed a preliminary analytical approach to the design of decentralized detection schemes for scenarios with spatially nonconstant binary phenomena, that is, phenomena with status (either "0" or "1") which may vary from sensor to sensor. We have also derived MMSE detection algorithms at the access point (AP), considering different quantization strategies at the sensors. In order to make our approach practical, a simplified detection algorithm, with a computational complexity much lower than that of the MMSE detection rule, has been proposed.

In this paper, we extend the approach presented in [18] to network scenarios where the communication links between the sensors and the AP may be *noisy*. These links are modeled either as binary symmetric channels (BSCs) or as additive white Gaussian noise (AWGN) channels. In particular, we study the relative impacts of communication and observation noises on the system performance, evaluated in terms of (i) distance between estimated and true phenomena and (ii) probability of local status estimation error (LSEE). As will be shown in the following, the proposed simplified detection algorithm incurs a limited performance loss with respect to the MMSE algorithm, yet guaranteeing a remarkable complexity reduction. Finally, the robustness and complexity of the proposed algorithms are investigated.

The structure of this paper is the following. In Section 2, we give preliminaries on decentralized detection. In Section 3, we derive the optimum MMSE detection rules at the AP in a scenario with noisy communication links and multiedge phenomena. In Section 4, we propose a simplified detection algorithm in order to reduce the computational complexity of the proposed decentralized detection scheme. In Section 5, numerical results on the performance of the proposed detection algorithms are presented. Finally, concluding remarks are given in Section 6.

2. Preliminaries on Decentralized Detection

As anticipated in Section 1, we focus on a network scenario where the status of the phenomenon under observation is characterized by a number N_{bs} of "edges," that is, sensor positions where the phenomenon changes its status from "0" (e.g., absence of a critical gas) to "1" (e.g., presence of a critical gas) or vice versa. For the sake of simplicity, we assume that the status of the phenomenon is independent from sensor to sensor. The proposed approach, however, can be extended to take into account the presence of correlation between sensors. In general, the presence of correlation would limit the number of edges and, if properly exploited at the AP, improve the performance with respect to that obtained in the following. A pictorial description of the proposed scenario is given in Figure 1(c). In particular, we investigate the performance when the communication links between the sensors and the AP are *noisy*, that is, errors may be introduced during data transmission. Note that, under the assumption that the geographical positions are known, from the estimated edges' positions the real geographic structure of the phenomenon (e.g., area with gas leakage) can be immediately determined.

Denote the overall phenomenon status as $\mathbf{H} = [H_1, \ldots, H_N]$, where $H_i \in \{0, 1\}$ is the status at the ith sensor ($i = 1, \ldots, N$). The signal observed at the ith sensor can be expressed as

$$r_i = c_{\text{E},i} + n_i, \tag{1}$$

where

$$c_{\text{E},i} \triangleq \begin{cases} 0, & \text{if } H_i = 0, \\ s, & \text{if } H_i = 1, \end{cases} \tag{2}$$

and $\{n_i\}$ are additive observation noise samples. Assuming that the noise samples $\{n_i\}$ are independent with the same Gaussian distribution $\mathcal{N}(0, \sigma^2)$, the common signal-to-noise ratio (SNR) at the sensors can be defined as follows:

$$\text{SNR}_{\text{sensor}} = \frac{\left[\mathbb{E}\{c_{\text{E},i} \mid H_i = 1\} - \mathbb{E}\{c_{\text{E},i} \mid H_i = 0\}\right]^2}{\sigma^2} = \frac{s^2}{\sigma^2}. \tag{3}$$

Each sensor processes (through proper quantization) the observed signal and the value output by the ith sensor is denoted as $d_i \triangleq f_{\text{quant}}(r_i)$, where the function $f_{\text{quant}}(\cdot)$ depends on the specific quantization strategy. In the following, we consider (i) binary quantization and (ii) absence of quantization. The analytical framework in the case of multilevel quantization can be easily derived from that presented in [18] for a scenario with ideal communication links. Upon reception of the messages sent by the sensors, the goal of the AP is to estimate, through MMSE or simplified detection strategies, the status of the binary phenomenon $\mathbf{H}$. As reference performance indicator, we will consider the quadratic distance (simply referred to as "distance") D between the observed phenomenon $\mathbf{H}$ and its estimate $\hat{\mathbf{H}}$, that is,

$$D\left(\mathbf{H}, \hat{\mathbf{H}}\right) \triangleq \left|\mathbf{H} \oplus \hat{\mathbf{H}}\right|^2, \tag{4}$$

where the notation $\oplus$ stands for bit-by-bit EX-OR and $\hat{\mathbf{H}}$ is the estimated phenomenon. Given that $\boldsymbol{\alpha} = [\alpha_1, \ldots, \alpha_{N_{\text{bs}}}]$

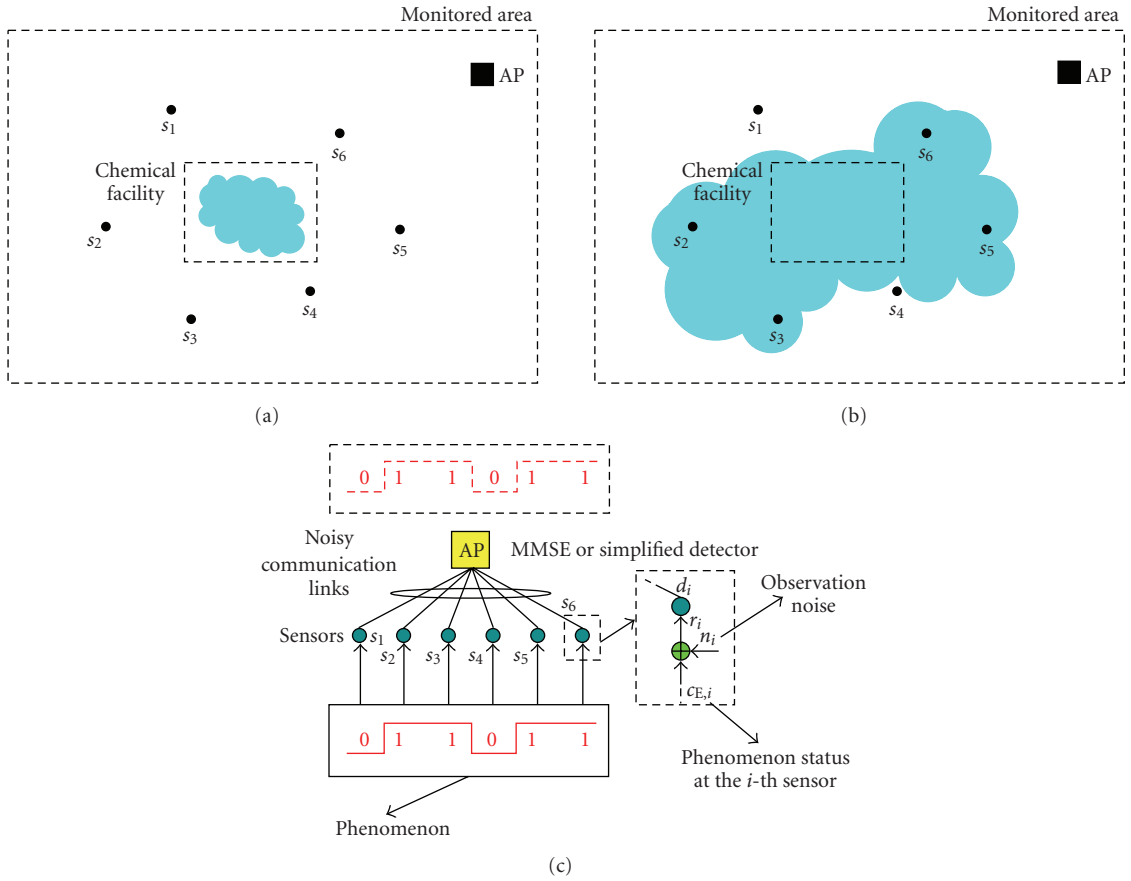

FIGURE 1: Illustrative scenario of interest: (a) a chemical facility processing dangerous gas; (b) scenario after gas leakage; (c) logical representation of the sensor network.

are the true edges' positions, $\hat{\mathbf{H}} = [\hat{H}_1, \ldots, \hat{H}_N]$ can be directly derived from the estimated edges' positions $\hat{\boldsymbol{\alpha}} = [\hat{\alpha}_1, \ldots, \hat{\alpha}_{N_{\text{bs}}}]$. Therefore, our goal is to accurately estimate $\boldsymbol{\alpha}$. The particular expression for $\hat{\boldsymbol{\alpha}}$ depends on the chosen distributed detection strategy, as will be shown in the following. We will also consider, as a meaningful performance indicator, the probability of LSEE, that is, the probability that the estimated phenomenon status at a sensor is wrong. In Section 5.2, it will be shown how the probability of LSEE is related to D.

3. MMSE One-Dimensional Edge Detection

The following assumptions are expedient to simplify the derivation of the MMSE one-dimensional edge detection strategy:

(i) the edges cannot be in correspondence to the first sensor and the last sensor: the number of edges must then be such that $1 \leq N_{\text{bs}} \leq N - 2$ (in particular, $H_N = H_{N-1}$);

(ii) the phenomenon status is perfectly known at the first sensor: without loss of generality, we assume $H_1 = 0$.

According to the above assumptions, the positions of the N_{bs} edges $\{\alpha_1, \ldots, \alpha_{N_{\text{bs}}}\}$ have to satisfy the following conditions:

$$2 \leq \alpha_1 < \alpha_2 < \cdots < \alpha_{k-1} < \alpha_k < \cdots < \alpha_{N_{\text{bs}}} \leq N - 1. \tag{5}$$

Therefore, between positions 1 and $\alpha_1 - 1$ the phenomenon status is "0," between positions α_1 and $\alpha_2 - 1$ the phenomenon status is "1," and so on. The following bound on the position of the kth edge must necessarily hold:

$$k + 1 < \alpha_k \leq (N - 1) - (N_{\text{bs}} - k) = N - N_{\text{bs}} + k - 1, \quad k = 1, \ldots, N_{\text{bs}}. \tag{6}$$

For each value of k, condition (6) formalizes the intuitive idea that the kth edge cannot fall beyond the $(N - 1 - N_{\text{bs}} + k)$th position, in order for the successive (remaining) $N_{\text{bs}} - k$ edges to have admissible positions.

In the remainder of this section, we derive the MMSE detection rules depending on the quantization strategy at the sensors.

3.1. Binary Quantization. In this scenario, the ith sensor makes a decision comparing its observation r_i with a

threshold value τ_i, and computes a local binary decision $d_i = f_{\text{quant}}(r_i) = U(r_i - \tau_i)$, where $U(\cdot)$ is the unit step function. To optimize the system performance, the thresholds $\{\tau_i\}$ need to be properly selected. In this paper, regardless of the value of N, a common value $\tau \simeq s/2$ at all sensors is considered [18].

In the presence of binary quantization at the sensors, the noisy communication links are modeled as BSCs. We denote as $\mathbf{d}$ the sequence of binary decisions at the sensors and $\mathbf{d}^{\text{AP}}$ as the sequence of binary decisions received at the AP. Under the assumption of BSCs, the received decisions $\mathbf{d}^{\text{AP}}$ might differ from $\mathbf{d}$ (there could be "bit-flipping" in some of the links). In particular, the ith decision received at the AP ($i = 1, \ldots, N$) can be expressed as

$$d_i^{\text{AP}} = \begin{cases} d_i, & \text{with probability } (1-p), \\ 1 - d_i, & \text{with probability } p, \end{cases} \tag{7}$$

where p is the cross-over probability of the BSC.

Theorem 1. *Assuming that N_{bs} is known at the AP and denoting by $\boldsymbol{\alpha} = (\alpha_1, \ldots, \alpha_{N_{bs}})$ the positions of the edges, the kth ($k = 1, \ldots, N_{bs}$) MMSE detected edge can be expressed as*

$$\hat{\alpha}_k = \sum_{\alpha_k = k+1}^{N - N_{bs} + k - 1} \alpha_k P\left(\alpha_k \mid \mathbf{d}^{AP}\right). \tag{8}$$

(For ease of notational simplicity, in (8) we use the same symbol α_k to denote both the random variable (in the second term) and its realization (in the third and fourth terms). This simplified notational approach will be considered in the remainder of Section 3. The context should eliminate any ambiguity.)

Proof. The MMSE detection strategy leads to the selection of the following vector of edges [19]:

$$\hat{\boldsymbol{\alpha}} = \mathbb{E}\left[\boldsymbol{\alpha} \mid \mathbf{d}^{\text{AP}}\right]. \tag{9}$$

The kth component ($k = 1, \ldots, N_{\text{bs}}$) of the vector $\hat{\boldsymbol{\alpha}}$ can then be written as

$$\hat{\alpha}_k = \mathbb{E}\left[\alpha_k \mid \mathbf{d}^{\text{AP}}\right] = \sum_{\alpha_k = 1}^{N} \alpha_k P\left(\alpha_k \mid \mathbf{d}^{\text{AP}}\right). \tag{10}$$

Taking into account the constraint (6), the upper and lower limits of the sum in (10) can be further refined, obtaining the right-hand side expression in (8). □

The computation of the conditional probabilities appearing at the right-hand side of (8) can be carried out as outlined in Appendix A.1.

3.2. Absence of Quantization. In this case, a local likelihood value, such as the conditional probability density function (PDF) of the observable, is transmitted from each sensor to the AP. Obviously, this is not a practical approach, since an infinite bandwidth would be required to transmit a PDF value. However, investigating this case allows to derive useful information about the limiting performance of the considered detection schemes, since transmission of the PDFs of the observables does not entail any information loss at the sensors. Note that this limiting performance can be achieved by using multilevel quantization at the sensors with an increasing number of quantization bits [18]. Since the sensors transmit real numbers (the likelihood values) to the AP, the BSC model for noisy communication links does not apply. In order to obtain results comparable with those associated with a scenario with binary quantization, we consider AWGN communication links. In other words, the ith observable at the AP ($i = 1, \ldots, N$), denoted as r_i^{AP}, can be written as

$$r_i^{\text{AP}} = r_i^{\text{sensor}} + n_i^{\text{comm}}, \tag{11}$$

where r_i^{sensor} is the observable transmitted by the ith sensor and n_i^{comm} has a Gaussian distribution $\mathcal{N}(0, \sigma^2_{\text{comm}})$. The value of σ^2_{comm} is set in order to make the AWGN scenario consistent with the BSC scenario. In particular, in the presence of uncoded binary phase shift keying (BPSK) transmission over AWGN links, the bit error rate is [20]

$$\text{BER} = Q\left(\sqrt{\frac{E_{\text{b}}}{\sigma^2_{\text{comm}}}}\right) \tag{12}$$

with $Q(x) \triangleq \int_x^\infty (1/\sqrt{2\pi}) \exp(-y^2/2) \mathrm{d}y$. Therefore, imposing that the BER in (12) is equal to the cross-over probability p of the equivalent BSC, the corresponding value of σ^2_{comm} can be obtained. This makes the performance comparison between the cases with binary quantization and without quantization consistent.

Theorem 2. *Assuming that N_{bs} is known at the AP, the kth ($k = 1, \ldots, N_{bs}$) MMSE detected edge can be recursively computed from*

$$\hat{\alpha}_k = \mathbb{E}\left[\alpha_k \mid \mathbf{r}^{AP}\right] = \sum_{\alpha_k = k+1}^{N - N_{bs} + k - 1} \alpha_k P\left(\alpha_k \mid \mathbf{r}^{AP}\right). \tag{13}$$

Proof. The proof follows exactly that of Theorem 1, but for replacing $\mathbf{d}^{\text{AP}}$ with $\mathbf{r}^{\text{AP}}$. □

The computation of the conditional probabilities appearing at the right-hand side of (13) can be carried out as outlined in Appendix A.2.

3.3. Remarks. We would like to remark that the MMSE strategy outlined above is based, regardless of the quantization strategy, on the assumption of knowledge of the number of edges N_{bs} at the AP. However, in the scenario of interest, for example, monitoring of a gas leakage, this knowledge may not be a priori available and N_{bs} should be properly estimated. In this case, by averaging over all possible realizations of N_{bs}, the average performance, with respect to the number of edges, could be determined. This extension goes beyond the scope of this paper. In fact, the performance of the MMSE algorithm with knowledge of N_{bs} at the AP will be used as a benchmark for the performance of the simplified (and feasible) one-dimensional edge detection algorithms introduced in Section 4.

4. Simplified One-Dimensional Edge Detection

Since the computational complexity of the MMSE detection strategy increases very quickly with the number of phenomenon edges (see Section 5.4 for more details), the derivation of a simplified distributed detection algorithm with low complexity (but limited performance loss) is crucial. As considered in Section 3 for MMSE detection, we distinguish between scenarios with binary quantization and without quantization.

4.1. Binary Quantization. Define the following "reconstruction" function:

$$f_{\mathrm{bq}}\left(k, \mathbf{d}_k^{\mathrm{AP}}, p\right) \triangleq (1-2p)\sum_{i=1}^{k}\left[P\left(H_i = 0 \mid d_i^{\mathrm{AP}}\right) - P\left(H_i = 1 \mid d_i^{\mathrm{AP}}\right)\right], \tag{14}$$

where $\mathbf{d}_k^{\mathrm{AP}} = (d_1^{\mathrm{AP}}, \ldots, d_k^{\mathrm{AP}})$ $(k = 1, \ldots, N)$ and the conditional probabilities $\{P(H_i = \ell \mid d_i^{\mathrm{AP}})\}$ are evaluated in Appendix B.1. The key idea of our approach is the following. While the phenomenon does not change its status, the function $f_{\mathrm{bq}}(k, \mathbf{d}_k^{\mathrm{AP}}, p)$ is a monotonically increasing (or decreasing) function of k. In correspondence to each change of the phenomenon status, the function $f_{\mathrm{bq}}(k, \mathbf{d}_k^{\mathrm{AP}}, p)$ changes its monotonic behavior. More precisely, a phenomenon variation from "0" to "1" corresponds to a change, trendwise, from increasing to decreasing; a phenomenon variation from "1" to "0" corresponds to a change, trendwise, from decreasing to increasing. Therefore, through the monotonicity changes of f_{bq} one can detect the positions of the edges. Moreover, since $p \in (0, 0.5)$ it follows that the term $(1-2p)$ is always positive and, therefore, can be neglected to study the monotonicity of f_{bq}. An illustrative example of the behavior of f_{bq} is shown in Figure 2, where the phenomenon under observation and the reconstruction function are shown, together with the detected edges. In this pictorial example, the estimated phenomenon coincides with the observed phenomenon.

4.2. Absence of Quantization. In the absence of quantization at the sensors, one can define the following reconstruction function:

$$f_{nq}\left(k, \mathbf{r}_k^{\mathrm{AP}}\right) \triangleq \sum_{i=1}^{k}\left[P\left(H_i = 0 \mid r_i^{\mathrm{AP}}\right) - P\left(H_i = 1 \mid r_i^{\mathrm{AP}}\right)\right] \tag{15}$$

where $\mathbf{r}_k^{\mathrm{AP}} = (r_1^{\mathrm{AP}}, \ldots, r_k^{\mathrm{AP}})$ $(k = 1, \ldots, N)$ and $\{P(H_i = \ell \mid r_i^{\mathrm{AP}})\}$ are computed in Appendix B.2. The edge detection algorithm at the AP is then identical to that presented in the case with binary quantization, but for the use of f_{nq} at the place of f_{bq}.

4.3. Remarks. One should observe that, unlike the MMSE strategy, our simplified edge detection algorithm (with binary quantization and no quantization, resp.) does *not* require knowledge of the number of edges N_{bs} at the AP. Therefore, the simplified algorithm is suitable for area monitoring applications, since in this scenario N_{bs} is not a priori known. Obviously, we expect that the proposed algorithm will incur a performance degradation with respect to the MMSE algorithm. However, this loss will be limited, as shown with simulation results in Section 5.

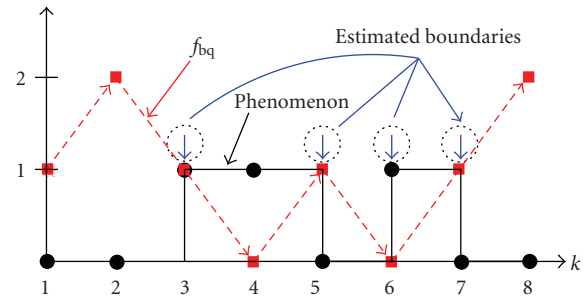

FIGURE 2: Illustrative example: the phenomenon under observation (solid line with circles) and the corresponding reconstruction function f_{bq} in (14) (dashed arrows). The estimated edges are indicated by vertical arrows.

5. Numerical Results

5.1. Performance Analysis: Distance. The performance of the proposed detection schemes is first analyzed by evaluating of the distance $D = D(\mathbf{H}, \hat{\mathbf{H}})$ between the true phenomenon $\mathbf{H}$ and the estimated phenomenon $\hat{\mathbf{H}}$. More precisely, the Monte Carlo simulation results are obtained through the following steps:

(1) the number of edges is randomly generated—the AP is assumed to know this number in the MMSE case;

(2) for a selected number of edges, their positions are randomly generated (From an operative viewpoint, in a scenario where the number of edges is larger than one, after the position of an edge is extracted, the following edge position is randomly chosen among the remaining positions. After all edges' positions are extracted, they are ordered.) ;

(3) either the sensors' decisions or the PDFs of the observables, according to the chosen quantization strategy at the sensors, are transmitted to the AP;

(4) a noisy version of the transmitted data is received at the AP;

(5) the AP detects the edges' positions through either MMSE or simplified detection algorithms;

(6) the distance D is evaluated, on the basis of the detected sequence of edges' positions;

(7) steps (1) ÷ (6) are repeated for sufficiently large number of times in order to derive statistically meaningful results;

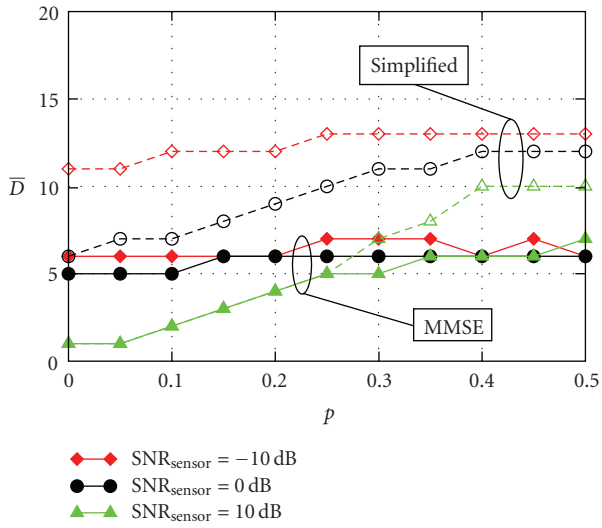

Figure 3: Distance, as a function of the cross-over probability p, in a scenario with $N = 8$ sensors and binary quantization. Three values for the sensor SNR are considered: (i) −10 dB, (ii) 0 dB, and (iii) 10 dB. Both MMSE and simplified detection algorithms at the AP are considered.

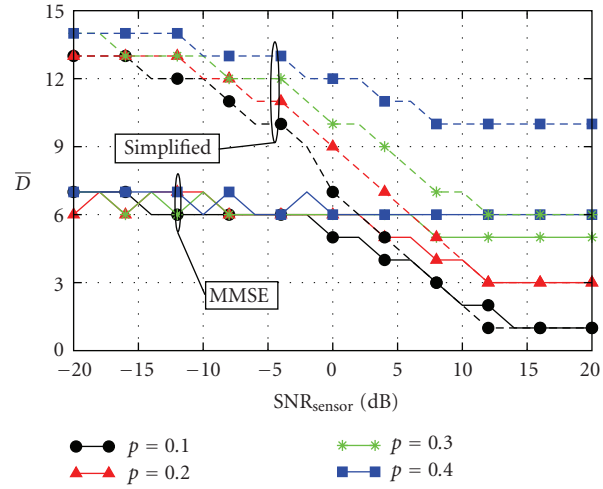

Figure 4: Distance, as a function of the sensor SNR, in a scenario with $N = 8$ sensors and binary quantization. Four different values of the cross-over probability p are considered: (i) 0.1, (ii) 0.2, (iii) 0.3, and (iv) 0.4. Both MMSE and simplified detection algorithms at the AP are considered.

(8) the average distance $\overline{D}$ is finally computed as the arithmetic average of the distances computed at the previous iterations (in step (6) at each iteration).

In Figure 3, the distance is shown, as a function of the cross-over probability p, in a scenario with $N = 8$ sensors and binary quantization—in this case, the communication links are modeled as BSCs. Three values for the sensor SNR are considered: (i) −10 dB, (ii) 0 dB, and (iii) 10 dB. Both MMSE and simplified detection algorithms at the AP are considered. As expected, the use of the simplified detection algorithm at the AP leads to a performance worse than that with the MMSE detection algorithm. However, the higher is the sensor SNR, the lower is the difference between the performance of the two algorithms. Moreover, one can observe that the distance might not converge to zero (as in the case with ideal communication links), due to the presence of two *independent* noise components (i.e., observation and communication noises). For a sufficiently large value of the sensor SNR, however, the distance reduces to zero when p tends to zero, in agreement with the results in [18].

In Figure 4, the distance $\overline{D}$ is shown, as a function of the sensor SNR, in a scenario with $N = 8$ sensors and binary quantization at the sensors. Four different values of the cross-over probability p are considered: (i) 0.1, (ii) 0.2, (iii) 0.3, and (iv) 0.4. The performance with both MMSE and simplified detection algorithms at the AP is investigated. Unlike the results presented in [18] for a scenario with ideal communication links, there appears to be a distance floor (higher than zero) for larger and larger values of the sensor SNR. This is to be expected, since the communication noise (independent of the observation noise at the sensors) prevents the AP from correctly recovering the data sent by the sensors. In particular, when the cross-over probability is sufficiently large (e.g., $p = 0.4$), the performance does not depend on the value of the sensor SNR, since the noisy communication links make the data sent by the sensors very unreliable, *regardless* of the observation quality. Finally, one can observe that, for small values of the sensor SNR, the simplified detection algorithm shows a nonnegligible performance loss with respect to the MMSE detection algorithm. However, this loss reduces to zero, for increasing values of the sensor SNR, *only* for sufficiently small values of p. In other words, if the communication links are not reliable, then increasing the accuracy of the observations at the sensors is useless.

In Figure 5 the distance $\overline{D}$ is shown, as a function of the sensor SNR, in a scenario with $N = 8$ sensors and absence of quantization—in this case, the noisy communication links are modeled as AWGN channels. Two different values of the bit error rate p (corresponding to different values of σ^2_{comm} according to (12)) are considered: (i) 0.1 and (ii) 0.2. The performance of both MMSE and simplified detection algorithms at the AP is evaluated. One can observe that, unlike the case with binary quantization at the sensors, the distance reduces to zero when the sensor SNR increases, that is, no floor appears. Moreover, the distance with the simplified detection rule at the AP approaches that with the MMSE detection rule, that is, it reduces to zero. This means that the proposed simplified detection algorithm is (asymptotically) effective. Obviously, this is only a theoretical performance limit. In fact, even if the communication links were noisy, the transmission of the "exact" observables (requiring an infinite bandwidth) from the sensors would allow a correct estimation of the true phenomenon. This cannot happen in realistic scenarios with limited transmission bandwidths.

In order to evaluate the loss incurred by the use of the simplified detection algorithm, it is expedient tointroduce

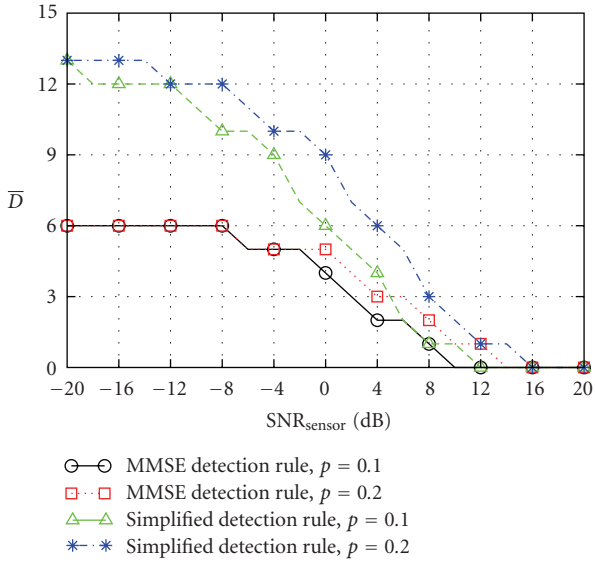

Figure 5: Distance, as a function of the sensor SNR, in a scenario with $N = 8$ sensors and absence of quantization. Two different values of the equivalent bit error rate p (corresponding to different values of σ^2_{comm} according to (12)) are considered: (i) 0.1 and (ii) 0.2. Both MMSE and simplified detection algorithms at the AP are considered.

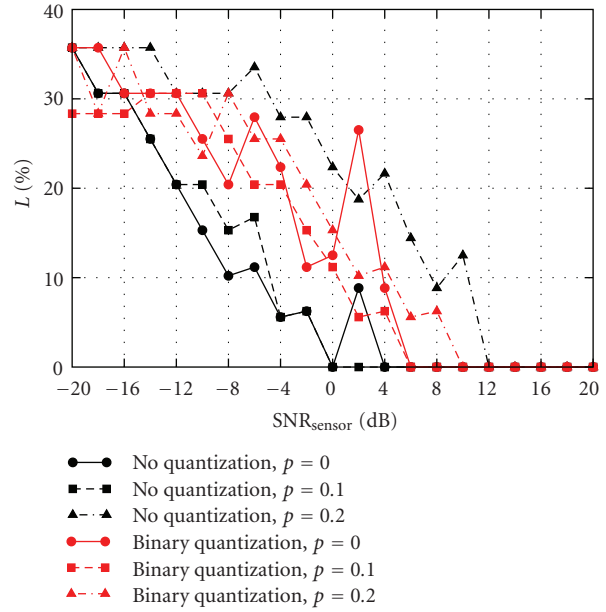

Figure 6: Percentage loss, as a function of the sensor SNR, in a scenario with $N = 8$ and simplified detection algorithm at the AP. Both absence of quantization and binary quantization at the sensors. Three values for p are considered: (i) 0 (ideal communication links), (ii) 0.1, and (iii) 0.2.

the following percentage loss:

$$L \triangleq \sqrt{\underbrace{\frac{\overline{D}^{\text{simp}} - \overline{D}^{\text{MMSE}}}{\overline{D}^{\text{MMSE}}}}_{\text{Term}_1} \cdot \underbrace{\frac{\overline{D}^{\text{simp}} - \overline{D}^{\text{MMSE}}}{N^2}}_{\text{Term}_2}}, \tag{16}$$

where $\overline{D}^{\text{simp}}$ and $\overline{D}^{\text{MMSE}}$ correspond to the distances obtained with the simplified and MMSE detection algorithms, respectively. The intuition behind the definition of L in (16), corresponding to the geometric average of Term_1 and Term_2, is the following. Term_1 represents the relative loss of the simplified detection rule with respect to the MMSE detection rule. However, using only this term could be misleading. In fact, for high sensor SNRs, the terms $\overline{D}^{\text{simp}}$ and $\overline{D}^{\text{MMSE}}$ are much lower than N^2 (the maximum possible distance). Therefore, even if $\overline{D}^{\text{simp}} > \overline{D}^{\text{MMSE}}$ (e.g., $\overline{D}^{\text{simp}} = 4$ and $\overline{D}^{\text{MMSE}} = 1$ with $N = 32$), both algorithms might perform very well. The introduction of Term_2 eliminates this ambiguity, since it represents the relative loss (between MMSE and simplified detection algorithms) with respect to the maximum (quadratic) distance, that is, N^2. In Figure 6, the behavior of L is shown, as a function of the sensor SNR, in a scenario with $N = 8$. In the region of interest ($\text{SNR}_{\text{sensor}} \geq 0$ dB), one can observe that L is lower than 20%, that is, the proposed simplified detection algorithm is effective.

In Figure 7(a), we investigate the distance, as a function of the cross-over probability p, in a scenario with binary quantization. Three values for the number of sensors are considered: (i) 16, (ii) 32, and (iii) 64. For each number of sensors, the sensor SNR assumes three possible values: (i) −10 dB, (ii) 0 dB, and (iii) 10 dB. In these scenarios, only the simplified detection algorithm is considered, since the computational complexity of the MMSE detection algorithm becomes unfeasible (see Section 5.4). In all cases, the distance is a monotonically nondecreasing function of p, but it might not converge to zero for $p \to 0^+$, because of the residual observation noise. For a sufficiently high value of the sensor SNR, however, the distance becomes very low when $p \to 0^+$, in agreement with the results in Figure 3. Moreover, note that for $p = 0.5$ the distance, for a given number of sensors, reaches the same value, regardless of the sensor SNR. This is due to the fact that, when $p = 0.5$, the AP receives "random" decisions and its estimate $\hat{\mathbf{H}}$ is extracted randomly among all possible ones for the corresponding number of edges. This limit (for $p = 0.5$), denoted as $\overline{D}_{\text{rand}}$, depends only on N and in Appendix C we derive a simple analytical approximation for it.

In order to better understand the impacts of the communication and observation noises, it is expedient to normalize, sensor SNR by sensor SNR, $\overline{D} = \overline{D}(\text{SNR}_{\text{sensor}}, p, N)$ by $\overline{D}_{\text{rand}}(N)$. In this way, the normalized distance $\overline{D}/\overline{D}_{\text{rand}}$, denoted as $\overline{D}_{\text{norm}} = \overline{D}_{\text{norm}}(\text{SNR}_{\text{sensor}}, p, N)$, assumes values in $[0, 1]$ and allows to directly compare scenarios with different numbers of sensors. The normalized versions of the distance curves of Figure 7(a) are shown in Figure 7(b). Obviously, when $p = 0.5$ the distance goes to the same value (i.e., 1), regardless of the values of N and $\text{SNR}_{\text{sensor}}$. As expected, for a given value of p (i.e., the communication quality), the higher the sensor SNR is (i.e., the observation quality) the more pronounced is the performance degradation for increasing values of N.

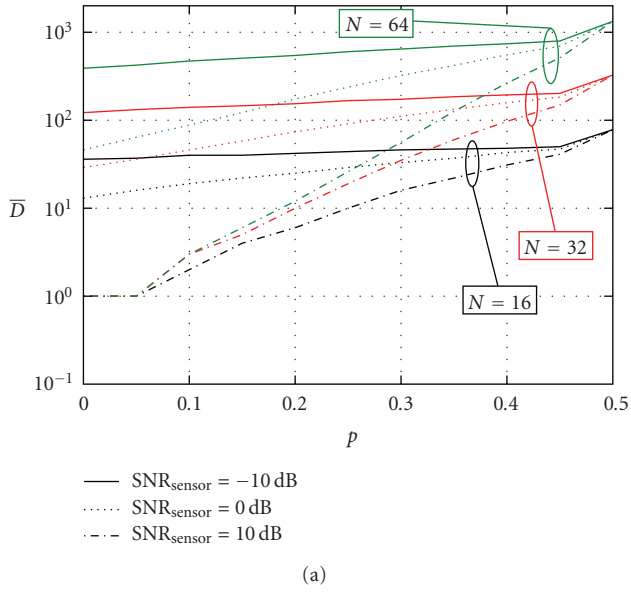

(a)

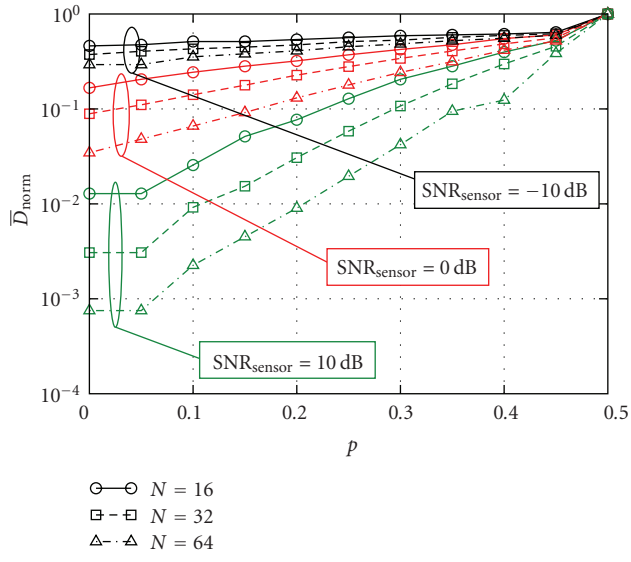

(b)

Figure 7: Distance, as a function of the cross-over probability p, in a scenario with binary quantization and simplified detection algorithm. Three values for the number of sensors are considered: (i) 16, (ii) 32, and (iii) 64. For a given number of sensors, three values for the sensor SNR are analyzed: (i) -10 dB, (ii) 0 dB, and (iii) 10 dB. In case (a), the distance is shown, whereas in case (b) the distance is normalized, for each value of N, to its corresponding maximum value ($\overline{D}(p = 0.5)$).

5.2. Performance Analysis: Probability of Local Status Estimation Error. Considering the same Monte Carlo simulation scenario described at the beginning of Section 5.1, the probability of LSEE can be approximated as follows:

$$P_{\mathrm{LSEE}} \simeq \frac{1}{N_{\mathrm{trials}}} \sum_{i=1}^{N_{\mathrm{trials}}} P_{\mathrm{LSEE}}^{(i)}, \tag{17}$$

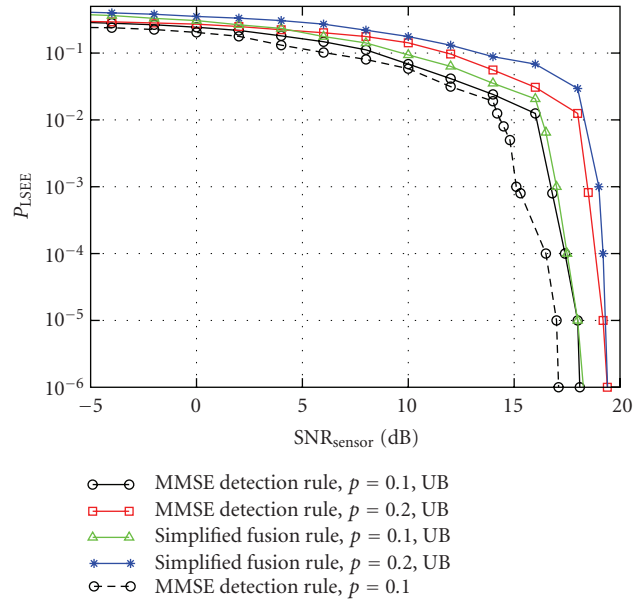

Figure 8: Probability of LSEE, as a function of the sensor SNR, for the same cases shown in Figure 5. For the MMSE case with $p = 0.1$, the exact performance and the UB are shown. For the other cases, only the UBs are shown.

where N_{trials} is the number of simulation runs, and $P_{\mathrm{MD}}^{(i)}$ is the probability of LSEE at the ith simulation run and can be written as

$$P_{\mathrm{LSEE}}^{(i)} \simeq \frac{\sqrt{D_i}}{N}, \tag{18}$$

where D_i is the distance at the ith simulation run. It then follows:

$$\begin{aligned} P_{\mathrm{LSEE}} &\simeq \frac{1}{N_{\mathrm{trials}}} \sum_{i=1}^{N_{\mathrm{trials}}} \frac{\sqrt{D_i}}{N} \\ &= \frac{1}{N} \frac{\sum_{i=1}^{N_{\mathrm{trials}}} \sqrt{D_i}}{N_{\mathrm{trials}}} \\ &\underset{N_{\mathrm{trials}} \to \infty}{\longrightarrow} \frac{1}{N} \overline{\sqrt{D}}. \end{aligned} \tag{19}$$

Observing that $\sqrt{\cdot}$ is a concave function and by using the Jensen inequality [21], one can write

$$\overline{\sqrt{D}} = \mathbb{E}\left[\sqrt{D}\right] \leq \sqrt{\mathbb{E}[D]} = \sqrt{\overline{D}}. \tag{20}$$

Therefore, the probability of LSEE can be upper bounded as follows:

$$P_{\mathrm{LSEE}} \lesssim \frac{\sqrt{\overline{D}}}{N}. \tag{21}$$

In other words, the evaluation of the average distance $\overline{D}$ allows to directly derive un upper bound (UB) on the probability of LSEE. In Figure 8, the probability of LSEE is shown, as a function of the sensor SNR, for the same cases

shown in Figure 5 (note that similar considerations hold for all other scenarios considered in Section 5.1). For the sake of graphical clarity, the exact performance is reported only for the scenario with the MMSE detection rule and $p = 0.1$. However, in all cases the maximum SNR distance between the UB and the true curve is less than 2 dB (for $P_{\text{LSEE}} \leq 10^{-2}$). From the results in Figure 8, a bimodal behavior of the probability of LSEE can be observed. In fact, this probability decreases very slowly, for increasing SNRs, till a value around 10^{-2}, below which it drops very rapidly to zero. The knee of the probability of LSEE is placed at an SNR which depends on the chosen detection (MMSE or simplified) strategy and on the communication noise level. Note that at very low SNR the probability of LSEE tends to be 0.5, that is, it randomly decides on the phenomenon status at each sensor.

5.3. System Robustness. We now investigate the robustness of the proposed simplified distributed detection algorithm with respect to possible mismatches between the actual system parameters and the used ones. In particular, we focus on a scenario with binary quantization at the sensors. Our conclusions hold also in other scenarios with different quantization strategies. In order to investigate the system robustness, we consider possible mismatches in the observation and communication phases, respectively.

(i) In the observation phase, we assume that there could be an error in the decision threshold used at each sensor. More precisely, denoting by $\overline{\tau}$ the optimized decision threshold ($\overline{\tau} \simeq /2$), we assume that each sensor makes use of an actual decision threshold which is uniformly distributed in $[\overline{\tau} - \eta_o\overline{\tau}, \overline{\tau} + \eta_o\overline{\tau}]$, where $\eta_o \in [0, 1]$. The decision thresholds at different sensors are supposed to be independent.

(ii) In the communication phase, we assume that, while the detection algorithm at the AP assumes a constant cross-over probability (denoted as $\overline{p}$) for all communication links, the actual cross-over probabilities in the various links are independent and uniformly distributed in the $[\overline{p}-\eta_c\overline{p}, \overline{p}+\eta_c\overline{p}]$, where $\eta_c \in [0, 1]$.

For the sake of simplicity, we consider a scenario with $N = 8$ sensors, binary quantization at the sensors, and simplified detection rule at the AP. In Figure 9, we show the performance results, in terms of distance versus (a) η_o and (b) η_c, in the presence of mismatches in the (a) observation phase and (b) communication phases, respectively. In case (a), three values of the cross-over probability p of the communication links are considered: (i) 0, (ii) 0.2, and (iii) 0.5. In case (b), three values are considered for the *average* cross-over probability $\overline{p}$: (i) 0.1, (ii) 0.2, and (iii) 0.5. For each value of p or $\overline{p}$, three values for the sensor SNR are considered: (i) −10 dB, (ii) 0 dB, and (iii) 10 dB.

In case (a), one can observe that, for sufficiently high values of the communication noise intensity p, there is a performance degradation (i.e., the distance increases) for increasing observation threshold mismatch (i.e., for increasing values of η_o), regardless of the sensor SNR. On the other hand, for low values of the communication noise intensity p and very high values of the sensor SNR (e.g., $\text{SNR}_{\text{sensor}} = 10$ dB), for increasing values of η_o the distance slightly increases. Finally, for low values of the communication noise intensity p and low/medium values of the sensor SNR, the distance slightly decreases for increasing values of η_o—this is due to the fact that in the presence of strong observation noise, the considered local decision strategy is no longer optimized. In all possible situations, the distance saturates at $\eta_o = 0.1$. In other words, the proposed simplified detection strategy is robust against local decision threshold mismatches.

In case (b), instead, the decision threshold τ at the sensors is fixed to $s/2$. As one can see, for high values of $\overline{p}$,

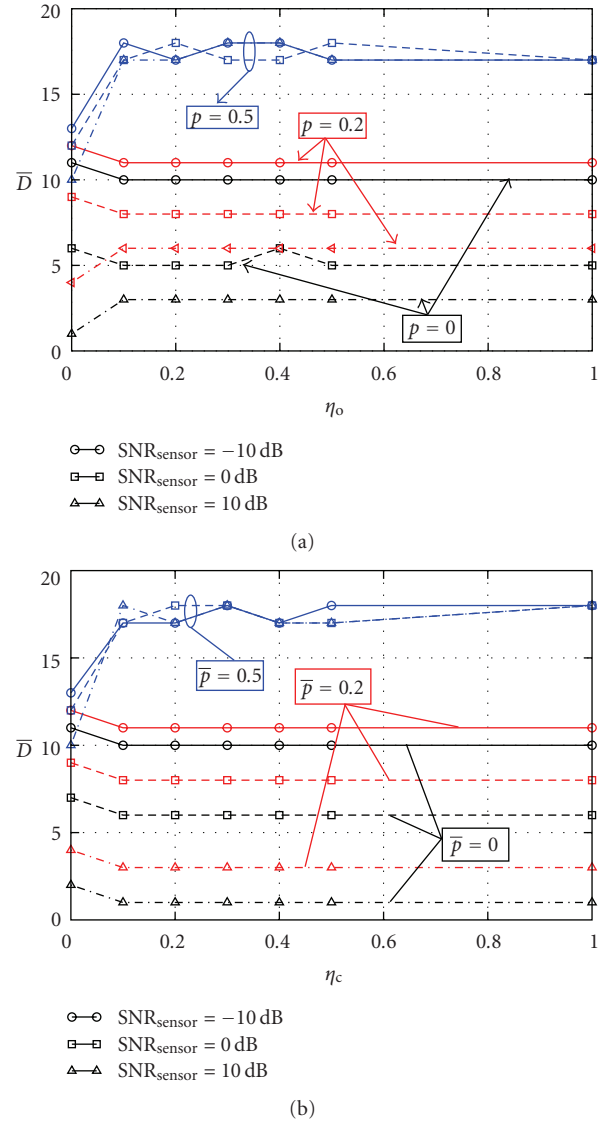

FIGURE 9: Distance, as a function of (a) η_o and (b) η_c, in the presence of mismatches in the (a) observation phase and (b) communication phases, respectively. In all cases, we consider $N = 8$ sensors, binary quantization at the sensors, and simplified detection rule at the AP. Various combinations of the values of p (in case (a)), $\overline{p}$ (in case (b)), and the sensor SNR are considered.

for increasing variability of the communication link quality (i.e., for increasing values of η_c) the performance rapidly degrades. For low values of $\overline{p}$, for increasing η_c there is a slight decrease of the distance, that is, a slight performance improvement—as previously commented, this depends on the fact that local sensor decision and AP detection strategies are no longer optimized. As in case (a), the performance with any scheme saturates at $\eta_c = 0.1$, that is, the proposed simplified detection rule is robust also against mismatches in the communication phase.

As a final remark, we point out that the fact that the proposed simplified detection rule is insensitive to strong fluctuations of the observation and communication qualities means that the system performance basically depends on the *average* observation and communication conditions.

5.4. Computational Complexity. Finally, we evaluate the improvement, in terms of computational complexity reduction with respect to the MMSE detection rule, brought by the use of the simplified detection algorithms. As complexity indicators, we choose the numbers of additions and multiplications (referred to as N_s and N_m, resp.) required by the considered detection algorithms, evaluated as functions of the number of sensors N. In a scenario with noisy communication links, the same considerations carried out in [18] for a scenario with ideal communication links still hold. In fact, the structures of the proposed detection algorithms are the same in both scenarios, since only the expressions of the used probabilities and PDFs change. Therefore, it can be shown that the numbers of additions and multiplications required by the MMSE detection algorithm would be $N_s^{\text{opt}} = \Theta(N^{N-2})$ and $N_m^{\text{opt}} = \Theta(N^{N-1})$. On the other hand, the computational complexity of the proposed simplified detection algorithm is characterized by $N_m^{\text{sub-opt}} = 0$ and $N_s^{\text{sub-opt}} = N$, showing a significant complexity reduction with respect to the MMSE detection algorithm—this also justifies the performance loss at small values of the sensor SNR.

6. Concluding Remarks

In this paper, we have analyzed the problem of one-dimensional edge detection in wireless sensor networking scenarios with noisy communication links. This situation arises in many practical applications such as those where an area of interest needs to be actively monitored to detect the presence of a phenomenon, for example, the presence of a gas leakage. We have proposed an analytical framework considering two quantization strategies at the sensors: (i) no quantization at the sensors and (ii) binary quantization. In each case, the MMSE detection algorithm at the AP has been derived and the impacts of relevant network parameters (e.g., the sensor SNR, the communication noise level, and the number of sensors) have been investigated. Then, a low-complexity and feasible detection algorithm, which does not require any a priori information on the number of edges, has been derived. We have shown that the performance penalty induced by the use of the simplified detection algorithms is asymptotically (for high sensor SNR and low communication noise level) negligible. Moreover, the simplified detection algorithm has proved to be robust against system parameters' variations. Finally, we have quantified the relevant computational complexity reduction brought by the use of the simplified detection algorithms with respect to the MMSE ones.

Appendices

A. Details on the MMSE Distributed Detection Strategy

A.1. Binary Quantization. The probability $P(\alpha_k \mid \mathbf{d})$ ($k = 1, \ldots, N_{\text{bs}}$) can be obtained by marginalizing the joint probabilities of the edges' positions as follows:

$$P\left(\alpha_k \mid \mathbf{d}^{\text{AP}}\right) = \sum_{\alpha_1} \cdots \sum_{\alpha_{k-1}} \sum_{\alpha_{k+1}} \cdots \sum_{\alpha_n} P\left(\boldsymbol{\alpha} \mid \mathbf{d}^{\text{AP}}\right) = \sum_{\boldsymbol{\alpha}:\alpha_k} P\left(\boldsymbol{\alpha} \mid \mathbf{d}^{\text{AP}}\right), \tag{A.1}$$

where $k = 1, \ldots, N_{\text{bs}}$ and the notation $\boldsymbol{\alpha} : \alpha_k$ indicates all sequences $\boldsymbol{\alpha}$ with α_k at the kth position.

At this point, one needs to evaluate the joint conditional probability mass functions (PMFs) at the right-hand side of (A.1). By applying the Bayes formula and the total probability theorem [22], after a few manipulations one obtains

$$P\left(\boldsymbol{\alpha} \mid \mathbf{d}^{\text{AP}}\right) = P\left(\mathbf{d}^{\text{AP}} \mid \boldsymbol{\alpha}\right) P(\boldsymbol{\alpha}) \times \left[\sum_{\alpha_1=2}^{N-N_{\text{bs}}} \cdots \sum_{\alpha_k=k+1}^{N-N_{\text{bs}}+k-1} \cdots \sum_{\alpha_{N_{\text{bs}}}=N_{\text{bs}}+1}^{N-1} P(\mathbf{d}^{\text{AP}} \mid \boldsymbol{\alpha}) P(\boldsymbol{\alpha}) \right]^{-1}. \tag{A.2}$$

We now characterize the three multiplicative terms at the right-hand side of (A.2). The first multiplicative term at the right-hand side of (A.2) can be written as

$$P\left(\mathbf{d}^{\text{AP}} \mid \boldsymbol{\alpha}\right) = \prod_{i=1}^{N} P\left(d_i^{\text{AP}} \mid \boldsymbol{\alpha}\right) = \prod_{i_0=1}^{\alpha_1-1} \underbrace{P(d_{i_0}^{\text{AP}} \mid \boldsymbol{\alpha})}_{H_{i_0}=0} \prod_{i_1=\alpha_1}^{\alpha_2-1} \underbrace{P(d_{i_1}^{\text{AP}} \mid \boldsymbol{\alpha})}_{H_{i_1}=1} \cdots \prod_{i_{N_{\text{bs}}}=\alpha_{N_{\text{bs}}}}^{N} \underbrace{P(d_{i_{N_{\text{bs}}}}^{\text{AP}} \mid \boldsymbol{\alpha})}_{H_{i_{N_{\text{bs}}}}=0 \text{ or } 1}, \tag{A.3}$$

where we have used the fact that the sensors' decisions are conditionally independent. Note that $H_{i_{N_{\text{bs}}}} = 0$ if N_{bs} is *even*, whereas $H_{i_{N_{\text{bs}}}} = 1$ if N_{bs} is *odd*. The component conditional

probabilities at the right-hand side of (A.3) can be expressed as follows:

$$P\left(d_i^{\mathrm{AP}} \mid \boldsymbol{\alpha}\right) = \begin{cases} p + (1-2p)P\left(n_i \underset{d_i^{\mathrm{AP}}=1}{\overset{d_i^{\mathrm{AP}}=0}{<}} \tau\right), & \text{if } i \in \mathcal{I}_0(\boldsymbol{\alpha}), \\ p + (1-2p)P\left(n_i \underset{d_i^{\mathrm{AP}}=1}{\overset{d_i^{\mathrm{AP}}=0}{>}} \tau - s\right), & \text{if } i \in \mathcal{I}_1(\boldsymbol{\alpha}), \end{cases} \tag{A.4}$$

where

$$\mathcal{I}_\ell(\boldsymbol{\alpha}) \triangleq \{\text{positions } \{i\} \text{ such that } H_i = \ell \mid \boldsymbol{\alpha}\} \quad \ell = 0, 1. \tag{A.5}$$

After a few manipulations, one obtains:

$$P\left(d_i^{\mathrm{AP}} \mid \boldsymbol{\alpha}\right) = \begin{cases} p + (1-2p)\Psi\left(d_i^{\mathrm{AP}}, \tau, \sigma, 0\right) & \text{if } i \in \mathcal{I}_0(\boldsymbol{\alpha}) \\ p + (1-2p)\Psi\left(d_i^{\mathrm{AP}}, \tau, \sigma, 1\right) & \text{if } i \in \mathcal{I}_1(\boldsymbol{\alpha}), \end{cases} \tag{A.6}$$

where

$$\Psi\left(d_i^{\mathrm{AP}}, \tau, \sigma, m\right) \triangleq \left(1 - d_i^{\mathrm{AP}}\right)\left[1 - Q\left(\frac{\tau - s \cdot m}{\sigma}\right)\right] + d_i^{\mathrm{AP}} Q\left(\frac{\tau - s \cdot m}{\sigma}\right) \tag{A.7}$$

with $Q(x) \triangleq \int_x^\infty (1/\sqrt{2\pi}) \exp(-y^2/2)\mathrm{d}y$.

The second multiplicative term at the right-hand side of (A.2) can be written, using the chain rule [22], as

$$P(\boldsymbol{\alpha}) = \prod_{i=1}^{N_{\mathrm{bs}}} P(\alpha_i \mid \alpha_{i-1}, \ldots, \alpha_1) = P(\alpha_1) \prod_{i=2}^{N_{\mathrm{bs}}} P(\alpha_i \mid \alpha_{i-1}), \tag{A.8}$$

where we have used the fact that the position of the ith edge depends only on the position of the (previous) $(i-1)$th edge. The multiplicative terms at the right-hand side of (A.8) can be evaluated by observing that each edge is spatially distributed according to the constraints in (6). In particular, by using combinatorics, it follows that

$$\begin{aligned} P(\alpha_1) &= \frac{1}{N - N_{\mathrm{bs}} + 1} \\ P(\alpha_k \mid \alpha_{k-1}) &= \frac{1}{N - N_{\mathrm{bs}} + k - \alpha_{k-1}} \quad k = 2, \ldots, N_{\mathrm{bs}}. \end{aligned} \tag{A.9}$$

The last term at the right-hand side of (A.2) (i.e., the denominator) can be easily computed by observing that it is composed of terms similar to those evaluated in (A.3) and (A.8).

A.2. Absence of Quantization. The conditional probabilities at the right-hand side of (13) can be obtained, as in Appendix A.1, through proper marginalization of joint conditional PMFs of the following type:

$$\begin{aligned} &P\left(\boldsymbol{\alpha} \mid \mathbf{r}^{\mathrm{AP}}\right) \\ &= p\left(\mathbf{r}^{\mathrm{AP}} \mid \boldsymbol{\alpha}\right) P(\boldsymbol{\alpha}) \\ &\quad \times \left[\sum_{\alpha_1=2}^{N-N_{\mathrm{bs}}} \cdots \sum_{\alpha_i+1}^{N-N_{\mathrm{bs}}+i-1} \cdots \sum_{\alpha_{N_{\mathrm{bs}}}=\alpha_{N_{\mathrm{bs}}-1}+1}^{N-1} p(\mathbf{r}^{\mathrm{AP}} \mid \boldsymbol{\alpha}) P(\boldsymbol{\alpha})\right]^{-1}. \end{aligned} \tag{A.10}$$

Since sensors' observations are independent, it holds that

$$p\left(\mathbf{r}^{\mathrm{AP}} \mid \boldsymbol{\alpha}\right) = \prod_{i=1}^{N} p\left(r_i^{\mathrm{AP}} \mid \boldsymbol{\alpha}\right), \tag{A.11}$$

where

$$\begin{aligned} p\left(r_i^{\mathrm{AP}} \mid \boldsymbol{\alpha}\right) &= \begin{cases} p_{\mathrm{comm}}\left(r_i^{\mathrm{AP}}\right), & \text{if } i \in \mathcal{I}_0(\boldsymbol{\alpha}), \\ p_{\mathrm{comm}}\left(r_i^{\mathrm{AP}} - s\right), & \text{if } i \in \mathcal{I}_1(\boldsymbol{\alpha}), \end{cases} \\ p_{\mathrm{comm}}(r) &\triangleq \frac{1}{\sqrt{2\pi(\sigma^2 + \sigma_{\mathrm{comm}}^2)}} \exp\left[-\frac{r^2}{2(\sigma^2 + \sigma_{\mathrm{comm}}^2)}\right]. \end{aligned} \tag{A.12}$$

One can notice that the effects of observation and communication AWGNs add directly.

B. Details on the Simplified One-Dimensional Edge Detection Strategy

B.1. Binary Quantization. The conditional PMFs $P(H_i = \ell \mid d_i^{\mathrm{AP}})$ $(\ell = 0, 1;\ i = 1, \ldots, N)$ in (14) can be written, by applying the Bayes formula, as

$$P\left(H_i = \ell \mid d_i^{\mathrm{AP}}\right) = \frac{P\left(d_i^{\mathrm{AP}} \mid H_i = \ell\right)}{P\left(d_i^{\mathrm{AP}} \mid H_i = 0\right) + P\left(d_i^{\mathrm{AP}} \mid H_i = 1\right)}, \tag{B.1}$$

where we have used the fact that $P(H_i = 0) = P(H_i = 1) = 1/2$ and

$$\begin{aligned} &P\left(d_i^{\mathrm{AP}} \mid H_i = \ell\right) \\ &= p + (1-2p)P\left(n_i \underset{d_i^{\mathrm{AP}}=1}{\overset{d_i^{\mathrm{AP}}=0}{<}} \tau - s \cdot \ell\right) \\ &= \left(1 - d_i^{\mathrm{AP}}\right)\left\{p + (1-2p)\left[1 - Q\left(\frac{\tau - s \cdot \ell}{\sigma}\right)\right]\right\} \\ &\quad + d_i^{\mathrm{AP}}\left[p + (1-2p)Q\left(\frac{\tau - s \cdot \ell}{\sigma}\right)\right]. \end{aligned} \tag{B.2}$$

B.2. Absence of Quantization. The conditional PMFs $\{P(H_i = \ell \mid r_i^{\mathrm{AP}})\}$ at the right-hand side in (15) can be computed as follows

$$P\left(H_i = \ell \mid r_i^{\mathrm{AP}}\right) = \frac{p_{\mathrm{comm}}\left(r_i^{\mathrm{AP}} - s \cdot \ell\right)}{p_{\mathrm{comm}}\left(r_i^{\mathrm{AP}}\right) + p_{\mathrm{comm}}\left(r_i^{\mathrm{AP}} - s\right)} \tag{B.3}$$

and $p_{\mathrm{comm}}(r)$ has been defined in Appendix A.2.

C. Limiting Distance for High Communication Noise

The limiting distance when $p = 0.5$ can be computed, by averaging over the possible (equiprobable) values for the number of edges N_{bs}, as

$$\overline{D}_{\text{rand}}(N) = \frac{1}{N-2} \sum_{N_{\text{bs}}=1}^{N-2} \overline{D}(N_{\text{bs}}), \tag{C.1}$$

where $\overline{D}(N_{\text{bs}})$ is the average distance in the presence of N_{bs} edges. The value of $\overline{D}(N_{\text{bs}})$ can in turn be computed by averaging over all possible pair-wise distances between the true phenomenon configurations and all possible configurations with N_{bs} edges for the (randomly) estimated phenomenon at the AP. We denote these sets of edges as $\{\boldsymbol{\alpha}_{\text{phen}}\}$ and $\{\boldsymbol{\alpha}_{\text{AP}}\}$, respectively. The distance between the phenomena (true and estimated) associated to a pair of these sequences is

$$D\left(N_{\text{bs}}, \boldsymbol{\alpha}_{\text{phen}}, \boldsymbol{\alpha}_{\text{AP}}\right) = D\left(\mathbf{H}\left(\boldsymbol{\alpha}_{\text{phen}}\right), \hat{\mathbf{H}}(\boldsymbol{\alpha}_{\text{AP}})\right). \tag{C.2}$$

The number of all possible sequences of N_{bs} edges can be computed by simply counting all possible configurations for the edges' positions, that is, as follows:

$$g(N_{\text{bs}}, N) = \sum_{\alpha_1=2}^{N-N_{\text{bs}}} \cdots \sum_{\alpha_k=k+1}^{N-N_{\text{bs}}+k-1} \cdots \sum_{\alpha_{N_{\text{bs}}}=N_{\text{bs}}+1}^{N-1} 1. \tag{C.3}$$

Therefore, one can write

$$\overline{D}(N_{\text{bs}}) = \frac{1}{g(N_{\text{bs}}, N)} \cdot \sum_{\{\boldsymbol{\alpha}_{\text{phen}}\}} \frac{1}{g(N_{\text{bs}}, N)} \sum_{\{\boldsymbol{\alpha}_{\text{AP}}\}} D\left(\mathbf{H}\left(\boldsymbol{\alpha}_{\text{phen}}\right), \hat{\mathbf{H}}(\boldsymbol{\alpha}_{\text{AP}})\right). \tag{C.4}$$

Finally, the limiting distance in (C.1) is

$$\overline{D}_{\text{rand}}(N) = \frac{1}{N-2} \sum_{N_{\text{bs}}=1}^{N-2} \frac{1}{\left[g(N_{\text{bs}}, N)\right]^2} \cdot \sum_{\{\boldsymbol{\alpha}_{\text{phen}}\}} \sum_{\{\boldsymbol{\alpha}_{\text{AP}}\}} D\left(\mathbf{H}\left(\boldsymbol{\alpha}_{\text{phen}}\right), \hat{\mathbf{H}}(\boldsymbol{\alpha}_{\text{AP}})\right). \tag{C.5}$$

The computation of the above expression is analytically very cumbersome. However, as shown in Figure 7 (a), it can be obtained out through simulations. In particular, our results show that an accurate approximation (through interpolation) is given by $\overline{D}_{\text{rand}}(N) \simeq \phi N^2$, where $\phi = 0.33$—in this case, the relative error between $\overline{D}_{\text{rand}}(N)$ and ϕN^2 is lower than 2.4% for $N \in \{8, \ldots, 512\}$.

Acknowledgment

The authors would like to thank Marco Sarti (Elettric 80 S.p.A., Viano, Reggio Emilia, Italy) for his help in the derivation of part of the simulator.

References

[1] I. F. Akyildiz, W. Su, Y. Sankarasubramaniam, and E. Cayirci, "A survey on sensor networks," *IEEE Communications Magazine*, vol. 40, no. 8, pp. 102–114, 2002.

[2] S. N. Simic and S. Sastry, "Distributed environmental monitorning using random sensor networks," in *Proceedings of the 2nd International Workshop on Information Processing in Sensor Networks*, pp. 582–592, Palo Alto, Calif, USA, April 2003.

[3] R. Viswanathan and P. K. Varshney, "Distributed detection with multiple sensors—part I: fundamentals," *Proceedings of the IEEE*, vol. 85, no. 1, pp. 54–63, 1997.

[4] I. Y. Hoballah and P. K. Varshney, "Information theoretic approach to the distributed detection problem," *IEEE Transactions on Information Theory*, vol. 35, no. 5, pp. 988–994, 1989.

[5] N. Gnanapandithan and B. Natarajan, "Joint optimization of local and fusion rules in a decentralized sensor network," *Journal of Communications*, vol. 1, no. 6, pp. 9–17, 2006.

[6] G. Ferrari and R. Pagliari, "Decentralized binary detection with noisy communication links," *IEEE Transactions on Aerospace and Electronic Systems*, vol. 42, no. 4, pp. 1554–1563, 2006.

[7] R. Nowak and U. Mitra, "Boundary estimation in sensor networks: theory and methods," in *Proceedings of the 2nd International Workshop on Information Processing in Sensor Networks*, pp. 80–95, Palo Alto, Calif, USA, April 2003.

[8] R. Nowak, U. Mitra, and R. Willett, "Estimating inhomogeneous fields using wireless sensor networks," *IEEE Journal on Selected Areas in Communications*, vol. 22, no. 6, pp. 999–1006, 2004.

[9] J. Barros and M. Tüchler, "Scalable decoding on factor trees: a practical solution for wireless sensor networks," *IEEE Transactions on Communications*, vol. 54, no. 2, pp. 284–294, 2006.

[10] Z.-Q. Luo, "An isotropic universal decentralized estimation scheme for a bandwidth constrained ad hoc sensor network," *IEEE Journal on Selected Areas in Communications*, vol. 23, no. 4, pp. 735–744, 2005.

[11] S. Duttagupta and K. Ramamritham, "Distributed boundary estimation using sensor networks," Tech. Rep., Indian Institute of Technology, Mumbai, India, 2006, http://www.it.iitb.ac.in/research/techreport/.

[12] S. Duttagupta, K. Ramamritham, and P. Ramanathan, "Distributed boundary estimation using sensor networks," in *Proceedings of the International Conference on Mobile Ad-hoc and Sensor Systems (MASS '06)*, pp. 316–325, Vancouver, Canada, October 2006.

[13] V. Torre and T. A. Poggio, "On edge detection," *IEEE Transactions on Pattern Analysis and Machine Intelligence*, vol. 8, no. 2, pp. 147–163, 1986.

[14] J. Canny, "A computational approach to edge detection," *IEEE Transactions on Pattern Analysis and Machine Intelligence*, vol. 8, no. 6, pp. 679–698, 1986.

[15] S. Konishi, A. L. Yuille, J. M. Coughlan, and C. Z. Song, "Statistical edge detection: learning and evaluating edge cues," *IEEE Transactions on Pattern Analysis and Machine Intelligence*, vol. 25, no. 1, pp. 57–74, 2003.

[16] A. Khashman, "Noise-dependent optimal scale in edge detection," in *Proceedings of the International Symposium on Industrial Electronics (ISIE '02)*, vol. 2, pp. 467–471, L'Aquila, Italy, July 2002.

[17] L. Jia and J. Xiaojun, "Edge detection based on decision-level information fusion and its application in hybrid image filtering," in *Proceedings of the International Conference on Image Processing (ICIP '04)*, vol. 1, pp. 251–254, Singapore, October 2004.

[18] G. Ferrari, M. Martalò, and M. Sarti, "Sensor networks as data acquisition devices—reduced-complexity decentralized detection of spatially non-constant phenomena," in *Grid Enabled Instrumentation and Measurement*, F. Davoli, N. Meyer, R. Pugliese, and S. Zappatore, Eds., Signals and Communication Technology, pp. 33–54, Springer, New York, NY, USA, 2008.

[19] S. M. Kay, *Fundamentals of Statistical Signal Processing, Volume I: Estimation Theory*, Prentice-Hall, Upper Saddle River, NJ, USA, 1993.

[20] J. G. Proakis, *Digital Communications*, McGraw-Hill, New York, NY, USA, 4th edition, 2001.

[21] T. M. Cover and J. A. Thomas, *Elements of Information Theory*, John Wiley & Sons, New York, NY, USA, 1991.

[22] A. Papoulis, *Probability, Random Variables and Stochastic Processes*, McGraw-Hill, New York, NY, USA, 1991.

Preliminary call for papers

The 2011 European Signal Processing Conference (EUSIPCO-2011) is the nineteenth in a series of conferences promoted by the European Association for Signal Processing (EURASIP, www.eurasip.org). This year edition will take place in Barcelona, capital city of Catalonia (Spain), and will be jointly organized by the Centre Tecnològic de Telecomunicacions de Catalunya (CTTC) and the Universitat Politècnica de Catalunya (UPC).

EUSIPCO-2011 will focus on key aspects of signal processing theory and applications as listed below. Acceptance of submissions will be based on quality, relevance and originality. Accepted papers will be published in the EUSIPCO proceedings and presented during the conference. Paper submissions, proposals for tutorials and proposals for special sessions are invited in, but not limited to, the following areas of interest.

Areas of Interest

- Audio and electro-acoustics.
- Design, implementation, and applications of signal processing systems.
- Multimedia signal processing and coding.
- Image and multidimensional signal processing.
- Signal detection and estimation.
- Sensor array and multi-channel signal processing.
- Sensor fusion in networked systems.
- Signal processing for communications.
- Medical imaging and image analysis.
- Non-stationary, non-linear and non-Gaussian signal processing.

Submissions

Procedures to submit a paper and proposals for special sessions and tutorials will be detailed at www.eusipco2011.org. Submitted papers must be camera-ready, no more than 5 pages long, and conforming to the standard specified on the EUSIPCO 2011 web site. First authors who are registered students can participate in the best student paper competition.

Important Deadlines:

Proposals for special sessions	15 Dec 2010
Proposals for tutorials	18 Feb 2011
Electronic submission of full papers	**21 Feb 2011**
Notification of acceptance	23 May 2011
Submission of camera-ready papers	6 Jun 2011

Webpage: www.eusipco2011.org

Organizing Committee

Honorary Chair
Miguel A. Lagunas (CTTC)

General Chair
Ana I. Pérez-Neira (UPC)

General Vice-Chair
Carles Antón-Haro (CTTC)

Technical Program Chair
Xavier Mestre (CTTC)

Technical Program Co-Chairs
Javier Hernando (UPC)
Montserrat Pardàs (UPC)

Plenary Talks
Ferran Marqués (UPC)
Yonina Eldar (Technion)

Special Sessions
Ignacio Santamaría (Unversidad de Cantabria)
Mats Bengtsson (KTH)

Finances
Montserrat Nájar (UPC)

Tutorials
Daniel P. Palomar (Hong Kong UST)
Beatrice Pesquet-Popescu (ENST)

Publicity
Stephan Pfletschinger (CTTC)
Mònica Navarro (CTTC)

Publications
Antonio Pascual (UPC)
Carles Fernández (CTTC)

Industrial Liaison & Exhibits
Angeliki Alexiou (University of Piraeus)
Albert Sitjà (CTTC)

International Liaison
Ju Liu (Shandong University-China)
Jinhong Yuan (UNSW-Australia)
Tamas Sziranyi (SZTAKI -Hungary)
Rich Stern (CMU-USA)
Ricardo L. de Queiroz (UNB-Brazil)